

# Ferroferric oxide nanoparticles induce prosurvival autophagy in human blood cells by modulating the Beclin 1/Bcl-2/VPS34 complex

Min Shi<sup>1,\*</sup>

Liang Cheng<sup>2,\*</sup>

Zubin Zhang<sup>1</sup>

Zhuang Liu<sup>2</sup>

Xinliang Mao<sup>1,3</sup>

<sup>1</sup>Jiangsu Key Laboratory of Translational Research and Therapy for Neuro-Psycho-Diseases, Department of Pharmacology, College of Pharmaceutical Sciences,

<sup>2</sup>Functional Nano and Soft Material (FUNSOM), Collaborative Innovation Center of Suzhou, Nano Science and Technology, <sup>3</sup>Jiangsu Key Laboratory of Preventive and Translational Medicine for Geriatric Diseases, Soochow University, Suzhou, People's Republic of China

\*These authors contributed equally to this study

Correspondence: Xinliang Mao  
Department of Pharmacology,  
Soochow University, 199 Ren Ai Road,  
Suzhou Industrial Park, Suzhou, 215123,  
People's Republic of China  
Tel +86 512 6588 2152  
Fax +86 512 6588 2152  
Email xinliangmao@suda.edu.cn

Zhuang Liu  
Functional Nano and Soft Material  
(FUNSOM), Soochow University,  
199 Ren Ai Road, Suzhou  
Industrial Park, Suzhou, 215123,  
People's Republic of China  
Tel +86 512 6588 2036  
Fax +86 512 6588 2036  
Email zliu@suda.edu.cn

**Abstract:** Magnetic iron oxide nanoparticles (NPs) are emerging as novel materials with great potentials for various biomedical applications, but their biological activities are largely unknown. In the present study, we found that ferroferric oxide nanoparticles ( $\text{Fe}_3\text{O}_4$  NPs) induced autophagy in blood cells. Both naked and modified  $\text{Fe}_3\text{O}_4$  NPs induced LC3 lipidation and degraded p62, a monitor of autophagy flux. And this change could be abolished by autophagy inhibitors. Mechanistically,  $\text{Fe}_3\text{O}_4$  NP-induced autophagy was accompanied by increased Beclin 1 and VPS34 and decreased Bcl-2, thus promoting the formation of the critical complex in autophagy initiation. Further studies demonstrated that  $\text{Fe}_3\text{O}_4$  NPs attenuated cell death induced by anticancer drugs bortezomib and doxorubicin. Therefore, this study suggested that  $\text{Fe}_3\text{O}_4$  NPs can induce prosurvival autophagy in blood cells by modulating the Beclin 1/Bcl-2/VPS34 complex. This study suggests that caution should be taken when  $\text{Fe}_3\text{O}_4$  NPs are used in blood cancer patients.

**Keywords:** iron oxide nanoparticle, autophagic pathway, anti-apoptosis

## Background

Magnetic iron oxide nanomaterials are a type of novel material that have raised extensive attention because of their great biocompatibility, biodegradability, and low toxicity.<sup>1,2</sup> With appropriate surface modifications, these materials have a promising potential for biomedicine, such as drug delivery, gene therapy, disease progress monitoring, and magnetic resonance imaging.<sup>1,2</sup> Ferroferric oxide ( $\text{Fe}_3\text{O}_4$ ) nanoparticles (NPs) are one such material displaying great potential for medical application; however, recent studies have demonstrated that these NPs might induce apoptosis and other cell responses.<sup>3</sup> It was reported that  $\text{Fe}_3\text{O}_4$  NP-induced apoptosis depends on the cell type. As a drug carrier, these NPs display very limited toxicity to cancer cell lines such as cervical cancer cells, but induce cytotoxicity and apoptosis in non-small lung cancer cells.<sup>3</sup> Moreover, this activity is probably associated with the surface modifications. A recent study showed that polyacrylic acid-coated but not naked  $\text{Fe}_3\text{O}_4$  NPs induce apoptosis.<sup>4</sup>

In addition to apoptosis, autophagy, another type of cell response, is frequently evoked in a self-protective manner in cells by foreign substances, such as drugs, or abnormal stress, such as irradiation and nutrient depletion.  $\text{Fe}_3\text{O}_4$  NPs induce autophagy in some cells such as lung epithelial cancer cells and human brain-derived endothelial cells.<sup>5,6</sup> But the biological responses of blood cancer cells to  $\text{Fe}_3\text{O}_4$  NPs are unclear. In the present study, we investigated the effects of  $\text{Fe}_3\text{O}_4$  NPs with various modifications on blood cells and found that  $\text{Fe}_3\text{O}_4$  NPs induce autophagy, which protects myeloma

cells from apoptosis induced by anticancer drugs. These results suggest caution should be taken when applying  $\text{Fe}_3\text{O}_4$  NPs in the blood system.

## Materials and methods

### Synthesis of $\text{Fe}_3\text{O}_4$ nanoparticles

In a typical procedure,<sup>7</sup> Tris(acetylacetonato) iron(III) or  $\text{Fe}(\text{acac})_3$  (2 mmol), 1,2-dexadecanediol (10 mmol), oleic acid (90%) (6 mmol), oleylamine (OM) (6 mmol), and benzyl ether (20 mL) were mixed and magnetically stirred under a flow of nitrogen. The mixture was heated to 200°C for 2 hours, and then heated to 300°C for 1 hour under a blanket of nitrogen. The black-colored mixture was cooled down to room temperature. Under the ambient conditions, ethanol (40 mL) was added to the mixture, and a black material was precipitated and separated via centrifugation. The black product was dissolved in hexane in the presence of oleic acid (~0.05 mL) and oleylamine (~0.05 mL). Then the product was precipitated with ethanol and centrifuged to remove the solvent. The bare  $\text{Fe}_3\text{O}_4$  nanoparticles were obtained for further application, such as surface modification.

### Synthesis of dopamine-polyacrylic acid-polyethylene glycol (DA-PAA-PEG) polymers

DA-PAA-PEG polymer was synthesized following a previous protocol.<sup>8</sup> Briefly, 18 mg PAA (mw=1,800, Sigma-Aldrich, 0.01 mmol) and 625 mg polyethylene glycol (PEG)- $\text{NH}_2$  (mw=5,000, Biomatrik Inc, 0.125 mmol) were dissolved in 2 mL dimethylformamide, into which 95.85 mg of 1-ethyl-3-(3-dimethylaminopropyl) carbodiimide hydrochloride (EDC, 0.5 mmol) and 104.5  $\mu\text{L}$  of triethylamine were added. The mixture was stirred for 24 hours at room temperature under the protection of nitrogen. After addition of 76.59 mg DA (Sigma-Aldrich, 0.5 mmol), 95.85 mg EDC (0.5 mmol) and 139  $\mu\text{L}$  triethylamine, the final mixture was stirred for another 24 hours under the same conditions. The obtained suspension was dialyzed against deionized water using dialysis membrane (molecular weight cutoff 10,000–14,000) for 24 hours. The solution was frozen dried, yielding the final product DA-PAA-PEG copolymer in a white solid.

### Synthesis of $\text{Fe}_3\text{O}_4$ nanoparticles modified with dopamine, dimercaptosuccinic acid, or DA-PAA-PEG

The methods for the preparation of these nanoparticles were described previously.<sup>7</sup> Briefly, DA (50 mg), dimercaptosuccinic

acid (DMSA) (50 mg), or DA-PAA-PEG (50 mg), dissolved in 1 mL of water, was slowly added into a tetrahydrofuran solution containing 200 mg bare  $\text{Fe}_3\text{O}_4$  nanoparticles under bath ultrasonication in 30 minutes. After stirring at room temperature for 3 hours, the solvent was removed by centrifugation at 15,000 rpm. These DA, DMSA, and DA-PAA-PEG modified  $\text{Fe}_3\text{O}_4$  NPs were referred to  $\text{Fe}_3\text{O}_4$ -DA,  $\text{Fe}_3\text{O}_4$ -DMSA, and  $\text{Fe}_3\text{O}_4$ -PEG, respectively.

### Transmission electronic microscopy and dynamic light scattering (DLS)

Morphology and sizes of the prepared  $\text{Fe}_3\text{O}_4$  NPs were characterized by transmission electronic microscopy (JEOL JEM-2100) as described previously.<sup>9</sup> Briefly, high-resolution transmission electron microscopy operated at accelerating voltages of 200 KV were used to determine morphology of NPs. DLS was applied to analyze the hydrodynamic diameter and zeta potentials on a ZetaPALS Analyzer (Brookhaven, NY).<sup>10</sup> The raw data were converted into zeta-potential values using the Helmholtz-Smoluchowski equation. The isoelectric point of nanoparticles in water was determined by measuring their zeta potentials and hydrodynamic diameter at the physiological pH condition.

### Cell culture

Human leukemia cell lines (K562 and OCI-AML2) and multiple myeloma (MM) cell lines (OPM2 and RPMI-8226) were purchased from American Type Culture Collection (Washington, DC). MM cell line JLN3 was a generous gift from Dr Aaron Schimmer (Ontario Cancer Institute, Toronto, Ontario, Canada). MM cells were cultured in Iscove's Modified Dulbecco's Medium (Thermo Scientific HyClone). Leukemia cells were maintained in RPMI-1640 media (HyClone). All media were supplemented with 10% of fetal bovine serum (Hyclone), 100 units/mL of penicillin and 100  $\mu\text{g}/\text{mL}$  of streptomycin.

### Antibodies and chemicals

Specific antibodies against light chain 3 (LC3), Beclin 1, p62, B-cell lymphoma 2 (Bcl-2), poly ADP-ribose polymerase (PARP), caspase-3, mammalian target of rapamycin (mTOR), phosphorylated mammalian target of rapamycin (p-mTOR), and phosphorylated protein kinase B were purchased from Cell signaling Technologies, Inc. (Danvers, MA). Antireduced glyceraldehyde-phosphate dehydrogenase (GAPDH) monoclonal antibody was purchased from Sigma (St Louis, MO). Bortezomib (BZ) was purchased from Santa Cruz, doxorubicin (Dox) and dexamethasone (Dex) were from

Sigma, bafilomycin A1 (BafA) and 3-methyladenine (3-MA) were purchased from Sigma-Aldrich. Chemoluminescence detection system and 4',6-diamidino-2-phenylindole (DAPI) were obtained from Beyotime Institute of Biotechnology, Nantong, People's Republic of China.

## Immunoblotting

Equal amounts (20 µg) of total proteins were denatured at 95°C for 5 minutes and then subjected to sodium dodecyl sulfate–polyacrylamide gel electrophoresis at a voltage of 120 V for 1.5 hours, followed by transfer to polyvinylidene difluoride membranes at 4°C in transfer buffer containing 0.1% sodium dodecyl sulfate and 20% methanol for 1 hour, with a voltage of 85 V. The blots were then blocked with 5% nonfat milk for 2 hours before being incubated with specific primary antibodies overnight at 4°C. Concentrations of the antibodies except GAPDH were 0.5 µg/mL and the concentration of anti-GAPDH was 0.05 µg/mL. Secondary antibody incubation and detection of the protein signals were performed as described previously.<sup>11</sup>

## Immunofluorescence

OPM2 cells (2.5×10<sup>5</sup>) were plated in 12-well-plates and were treated with modified Fe<sub>3</sub>O<sub>4</sub> NPs with the concentration of 100 µg/mL for 9 hours; starvation treatment was used as a positive control and dimethyl sulfoxide (DMSO) treatment was used as a negative control. OPM2 cells were then collected in cold phosphate buffer solution and transferred to glass slides using cytospin (Thermo) by a centrifuge at 800 rpm for 5 minutes. Cells were then subject to immunofluorescence analysis by staining with an anti-LC3 antibody (10 µg/mL) using a protocol as described previously.<sup>12</sup> Before being analyzed on a confocal microscopy (Olympus), cells were incubated with DAPI (5 µg/mL) for 10 minutes. The wavelengths of excitation and emission (Ex/Em) for DAPI and fluorescein isothiocyanate (FITC) were 405/498 nm and 488/525 nm, respectively.<sup>12</sup>

## Studies in primary blood cells

Whole blood samples were collected in heparin-treated tubes from adult male mice (8 weeks old, 20–22 grams, provided by Shanghai Slac Laboratory Animal Co. Ltd., Shanghai, People's Republic of China). The mice were anaesthetized by an injection of 4% chloral hydrate. Nucleated cells were then isolated from whole blood samples by a gradient centrifugation using Ficoll agent (Sigma-Aldrich)<sup>13</sup> and subjected to incubation with Fe<sub>3</sub>O<sub>4</sub> NPs for 9 hours before being analyzed for the expression of LC3, Beclin 1, and Bcl-2 with specific antibodies.

## Results

### Characterization of surface-modified Fe<sub>3</sub>O<sub>4</sub> NPs

The sizes of synthesized Fe<sub>3</sub>O<sub>4</sub> NPs were determined by with transmission electronic microscopy. As shown in Figures 1A, B, and C, Fe<sub>3</sub>O<sub>4</sub> NPs coated with various modifications were uniformly dispersed, the average sizes of the particles were <10 nm. Further studies by DLS found the hydrodynamic sizes varied depending on the modifications. The average DLS sizes of DA- and DMSA- modified nanoparticles were 25±4 and 26±4 nm, respectively, while the PEG modification increased the average DLS size to 50±7 nm (Figure 1D). Zeta potentials of each type of Fe<sub>3</sub>O<sub>4</sub> NPs in water are shown in Figure 1E. As expected, the modification affected the surface charge. Compared with the Fe<sub>3</sub>O<sub>4</sub>-DA and Fe<sub>3</sub>O<sub>4</sub>-DMSA particles, the Fe<sub>3</sub>O<sub>4</sub>-PEG particles carried a relative low potential, which was consistent with our previous studies.<sup>7</sup> Further studies showed that these modified Fe<sub>3</sub>O<sub>4</sub> NPs could dissolve in different types of solutions including water, phosphate buffered saline (PBS), RPMI-1640 cell medium, and fetal bovine serum. All solutions exhibited excellent stability in all tested physiological solutions within 24 hours (Figures 1F–H).

### Fe<sub>3</sub>O<sub>4</sub> NPs induce autophagy in blood cancer cells

NPs are not toxic to many cell types, but recent investigations showed that they can induce apoptosis and/or autophagy in certain cells, such as lung cancer cells.<sup>6</sup> To find out whether the Fe<sub>3</sub>O<sub>4</sub> NPs induced autophagy in blood cancer cells, leukemia cell lines (OCI-AML2 and K562) and multiple myeloma (MM) cell lines (OPM2, 8226, JLN3) were treated with 100 µg/mL of Fe<sub>3</sub>O<sub>4</sub> NPs with specific modifications including DA, DMSA, or PEG for 9 hours. To view autophagy induced by Fe<sub>3</sub>O<sub>4</sub> NPs, the expression level of LC3-II, a phosphatidylethanolamine (PE)-conjugated form from microtubule-associated protein 1A/B-LC3 was measured because it is a common indicator of autophagy.<sup>14</sup> Immunoblotting suggested that LC3-II was induced in all cells treated with Fe<sub>3</sub>O<sub>4</sub> NPs (Figure 2A). This induction of LC3-II was in a time- and concentration-dependent manner (Figures 2B and C). LC3-II could be induced by Fe<sub>3</sub>O<sub>4</sub> NPs at a concentration as low as 12.5 µg/mL within 9 hours (Figure 2B), or within 3 hours at the 100 µg/mL of all three types of particles (Figure 2C). To further visualize whether increased LC3-II was lipidated to the autophagosome membrane, OPM2 cells were starved or treated with each type of Fe<sub>3</sub>O<sub>4</sub> NPs at 100 µg/mL for 9 hours,

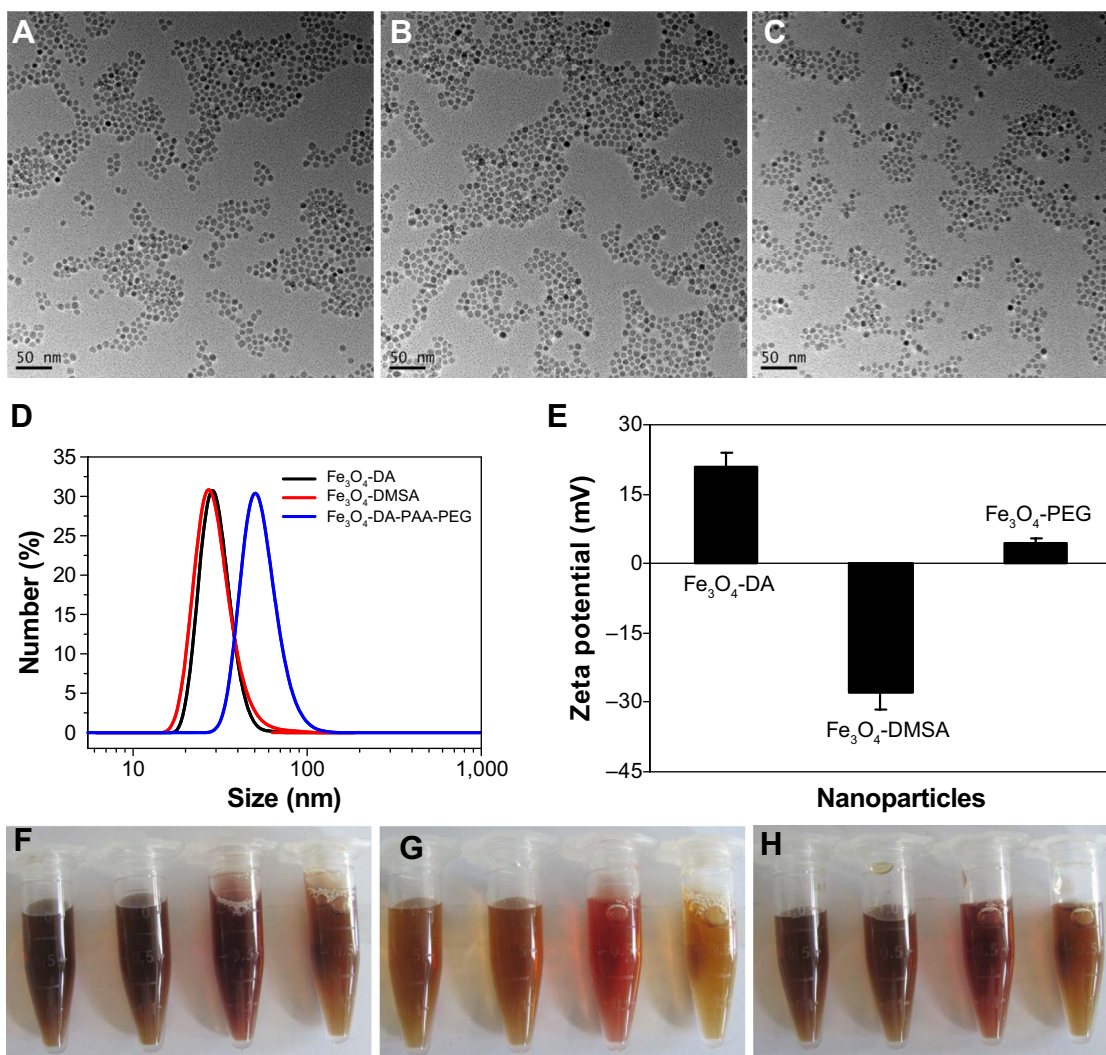


**Figure 1** Characterization of various surface modifications of superparamagnetic nanoparticles.

**Notes:** TEM images of (A)  $\text{Fe}_3\text{O}_4$ -DA, (B)  $\text{Fe}_3\text{O}_4$ -DMSA, and (C)  $\text{Fe}_3\text{O}_4$ -PEG. (D) DLS size of  $\text{Fe}_3\text{O}_4$ -DA,  $\text{Fe}_3\text{O}_4$ -DMSA, and  $\text{Fe}_3\text{O}_4$ -PEG in water solution; (E) Zeta potential of the  $\text{Fe}_3\text{O}_4$ -DA,  $\text{Fe}_3\text{O}_4$ -DMSA, and  $\text{Fe}_3\text{O}_4$ -PEG in water solution. Photos of (F)  $\text{Fe}_3\text{O}_4$ -DA, (G)  $\text{Fe}_3\text{O}_4$ -DMSA, and (H)  $\text{Fe}_3\text{O}_4$ -PEG in various solutions: water, phosphate buffered saline (PBS), RPMI-1640 cell medium, and fetal bovine serum (FBS) from left to right.

**Abbreviations:** DA, dopamine; DMSA, dimercaptosuccinic acid; DLS, dynamic light scattering;  $\text{Fe}_3\text{O}_4$ , ferroferric oxide; PEG, polyethylene glycol; TEM, transmission electronic microscopy.

followed by immunofluorescence staining.<sup>12</sup> As shown in Figure 2D, starvation, as predicted, led to increased LC3-II puncta appearing as green dots in the confocal microscope. Similar to starvation,  $\text{Fe}_3\text{O}_4$  NPs at all modifications also led to increased LC3-II puncta, a critical marker of autophagy.<sup>12,14</sup> Therefore,  $\text{Fe}_3\text{O}_4$  NPs probably induce autophagy in blood cancer cells.

### $\text{Fe}_3\text{O}_4$ NPs-induced autophagy is blocked by inhibitors of autophagy or lysosomes

It is well known that autophagy can be blocked by specific autophagy inhibitors or lysosome inhibitors.<sup>15</sup> To further

confirm  $\text{Fe}_3\text{O}_4$  NPs-induced autophagy, myeloma cell line OPM2 was treated with  $\text{Fe}_3\text{O}_4$  NPs alone or along with 3-MA, an inhibitor of autophagy, or bafilomycin A1 (BafA), a lysosome inhibitor.<sup>15</sup> As shown in Figure 3,  $\text{Fe}_3\text{O}_4$  NPs induced LC3-II and decreased p62. When 3-MA was added, the changes of LC3-II and p62 by  $\text{Fe}_3\text{O}_4$  NPs were abolished (Figures 3A, B, and C). In contrast, BafA increased the protein levels of both LC3-II and p62. Because p62 degradation is a hallmark of the autophagy flux and an important biomarker of autophagy,<sup>16</sup> the effects of 3-MA and BafA on the protein level of p62 further demonstrated that  $\text{Fe}_3\text{O}_4$  NPs-induced autophagy in blood cancer cells.

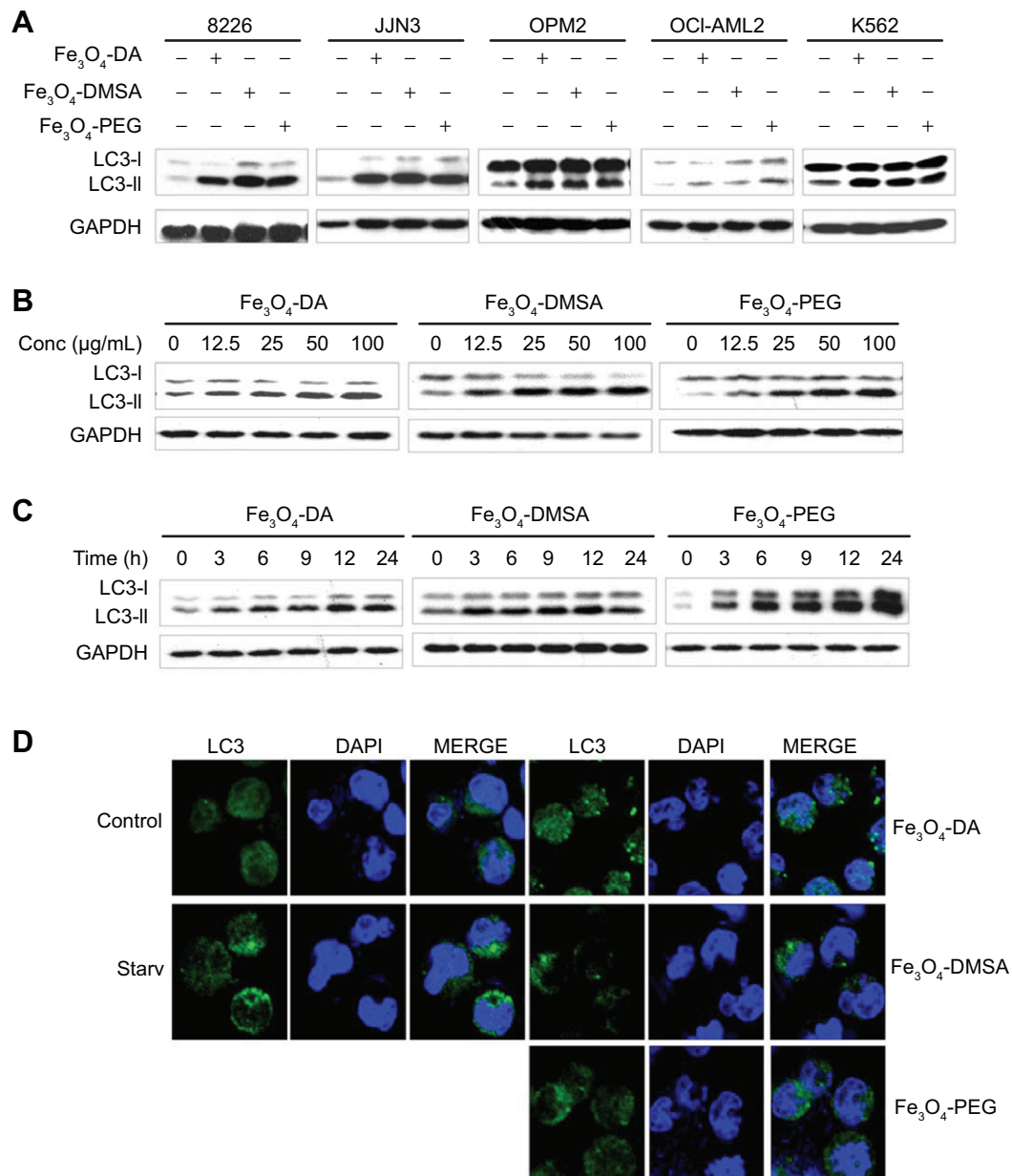


**Figure 2** Fe<sub>3</sub>O<sub>4</sub> NPs upregulate LC3-II expression and induce LC3 lipidation.

**Notes:** (A) Multiple myeloma cells (JJN3, 8226, OPM2) and leukemia cells (AML2 and K562) were treated with Fe<sub>3</sub>O<sub>4</sub> NPs with different surface modifications. LC3-II was evaluated by immunoblotting against a specific antibody. (B) LC3-II was induced in OPM2 cells by Fe<sub>3</sub>O<sub>4</sub> NPs in a concentration-dependent manner. (C) LC3-II was induced in OPM2 by Fe<sub>3</sub>O<sub>4</sub> NPs in a time-dependent manner. (D) Multiple myeloma cells OPM2 was treated with different Fe<sub>3</sub>O<sub>4</sub> NPs for 9 hours, followed by immunofluorescent analysis with a specific antibody against LC3-II. LC3-II puncta were observed by a confocal microscopy. Starvation (Starv.) was used as a positive control.

**Abbreviations:** DA, dopamine; DAPI, 4',6-diamidino-2-phenylindole; DMSA, dimercaptosuccinic acid; Fe<sub>3</sub>O<sub>4</sub>, ferroferric oxide; GAPDH, glyceraldehyde-phosphate dehydrogenase; LC3, light chain 3; MERGE, LC3 and DAPI; NPs, nanoparticles; PEG, polyethyleneglycol.

## Fe<sub>3</sub>O<sub>4</sub> NPs target the Beclin 1/VPS34/Atg14 complex

Autophagy is mediated by a series of important cell signaling pathways. Its initiation is triggered by nutrient depletion via the mTOR signaling, while the elongation of autophagosomes is mainly modulated by the Beclin 1/VPS34/autophagy-related gene (Atg14) complex.<sup>17</sup> To find out the mechanisms involved

in Fe<sub>3</sub>O<sub>4</sub> NPs-induced autophagy, we first evaluated the protein kinase B/mTOR signaling after Fe<sub>3</sub>O<sub>4</sub> NPs treatment for 9 hours in which time Fe<sub>3</sub>O<sub>4</sub> induced autophagy as shown in Figures 2 and 3. However, immunoblotting revealed that mTOR activation was not affected by Fe<sub>3</sub>O<sub>4</sub> NPs after this treatment (Figure 4A), suggesting the mTOR signaling pathway might not be a major target of these types of nanoparticles.

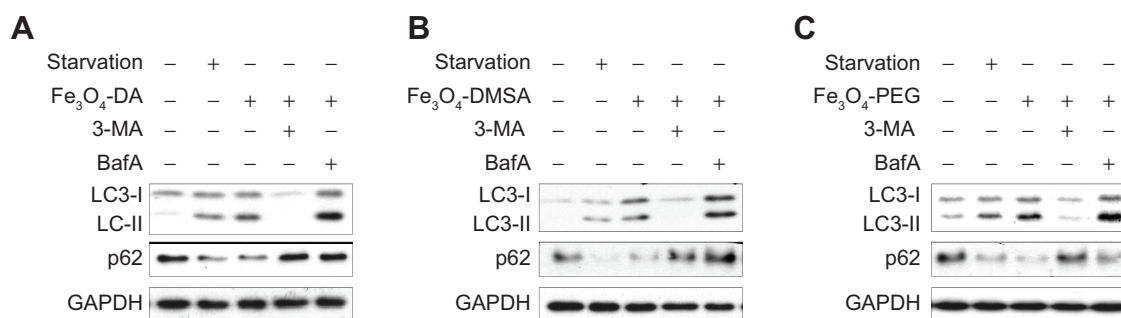


**Figure 3**  $\text{Fe}_3\text{O}_4$  NPs-induced autophagy is abrogated by autophagy inhibitors. OPM2 cells were treated for 9 hours by 100  $\mu\text{g}/\text{mL}$  of (A)  $\text{Fe}_3\text{O}_4$ -DA, (B)  $\text{Fe}_3\text{O}_4$ -DMSA, or (C)  $\text{Fe}_3\text{O}_4$ -PEG in the presence of 3-MA or BafA.

**Notes:** LC3-II accumulation and p62 degradation were measured by specific antibodies. Starvation was used as a positive control.

**Abbreviations:** 3-MA, 3-methyladenine; BafA, bafilomycin A1; Bcl-2, B-cell lymphoma 2; DA, dopamine; DMSA, dimercaptosuccinic acid;  $\text{Fe}_3\text{O}_4$ , ferroferric oxide; GAPDH, glyceraldehyde-phosphate dehydrogenase; LC3, light chain 3; NPs, nanoparticles; PEG, polyethyleneglycol.

Because 3-MA, an inhibitor of VPS34, blocked autophagy induced by  $\text{Fe}_3\text{O}_4$  NPs, it suggests that the VPS34 complex might play a key role in this autophagy. VPS34 acts by forming a complex with Beclin 1, Atg14, and other proteins to promote elongation of autophagosome;<sup>17</sup> therefore, we next evaluated the expression levels of the components in the VPS34 complex. Immunoblotting revealed that Beclin 1, VPS34, and Atg14 were induced while the Bcl-2, a negative modulator of Beclin 1, was decreased by these NPs (Figure 4B). And these changes were time- and concentration-dependent (Figures 4C and D). We next checked the protein levels of Atg14 and Beclin 1 after cells were treated for 3 to 24 hours and found that both Beclin 1 and Atg14 maintained a high level throughout this period, which was consistent with LC3-II expression. These results thus suggested the VPS34/Beclin 1 complex was important for  $\text{Fe}_3\text{O}_4$  NP-induced autophagy.

### $\text{Fe}_3\text{O}_4$ NPs prevent myeloma cell apoptosis induced by anticancer drugs

Autophagy has been proposed to deliver a survival or a death signal depending on the context and stress of cells.<sup>17</sup> To evaluate the effects of autophagy on cell apoptosis, we first measured cell proliferation in the presence of these chemically modified  $\text{Fe}_3\text{O}_4$  NPs. It showed that these  $\text{Fe}_3\text{O}_4$  NPs had no effects on cell proliferation even at a concentration up to 2 g/mL (data not shown). PARP and caspase-3, both of which are common hallmarks of cell apoptosis, were not cleaved by  $\text{Fe}_3\text{O}_4$  NPs at 100  $\mu\text{g}/\text{mL}$  (Figure 5A). To confirm the effects of these NPs on cell apoptosis, OPM2 cells were treated with antimyeloma drug BZ, Dex, or Dox. Among these three drugs, BZ was the most potent one and could activate marked apoptotic signaling evidenced by activated PARP and caspase-3 at a low nano concentration (Figures 5B, C, and D). Compared

with BZ, Dox and Dex were less potent; therefore, the cleaved form of caspase-3 was not markedly increased at current concentrations of Dex and Dox (Figures 5B, C, and D). In contrast, both cleaved PARP and caspase-3 in BZ-treated cells were markedly decreased by all three modified nanoparticles (Figure 5). Therefore, this experiment indicated that  $\text{Fe}_3\text{O}_4$  NP-induced autophagy probably exhibited an antiapoptotic or a prosurvival function at least in blood cancer cells.

### Bare $\text{Fe}_3\text{O}_4$ NPs induce prosurvival autophagy

Above studies demonstrated that these  $\text{Fe}_3\text{O}_4$  NPs with various chemical modifications were able to induce autophagy in blood cancer cells. We wondered whether these modifications might be important for the autophagy induced by these  $\text{Fe}_3\text{O}_4$  NPs. To find out, we next examined the effects of bare  $\text{Fe}_3\text{O}_4$  NPs on autophagy in the same cell line – OPM2. As shown in Figures 6A and B, bare  $\text{Fe}_3\text{O}_4$  NPs induced the expression of bo LC3-II and Beclin 1 in a concentration- and time-dependent manner. Similar to the chemically modified  $\text{Fe}_3\text{O}_4$  NPs, bare  $\text{Fe}_3\text{O}_4$  NPs also led to degradation of p62, which could be abrogated by the autophagy inhibitor 3-MA or lysosome inhibitor BafA (Figure 6C). Notably, these bare  $\text{Fe}_3\text{O}_4$  NPs also displayed antiapoptotic activity by decreasing the cleavage of caspase-3 and PARP (Figure 6D). Therefore, these studies showed that  $\text{Fe}_3\text{O}_4$  NPs induced autophagy probably independent of the surface modifications.

### $\text{Fe}_3\text{O}_4$ NPs induce autophagy in primary blood cells

Lastly, we questioned whether these  $\text{Fe}_3\text{O}_4$  NPs induce autophagy in healthy blood cells. To this end, myeloid and lymphoid cells isolated from mice were incubated with  $\text{Fe}_3\text{O}_4$  NPs for 9 hours. Similar to the effects of  $\text{Fe}_3\text{O}_4$  NPs on blood

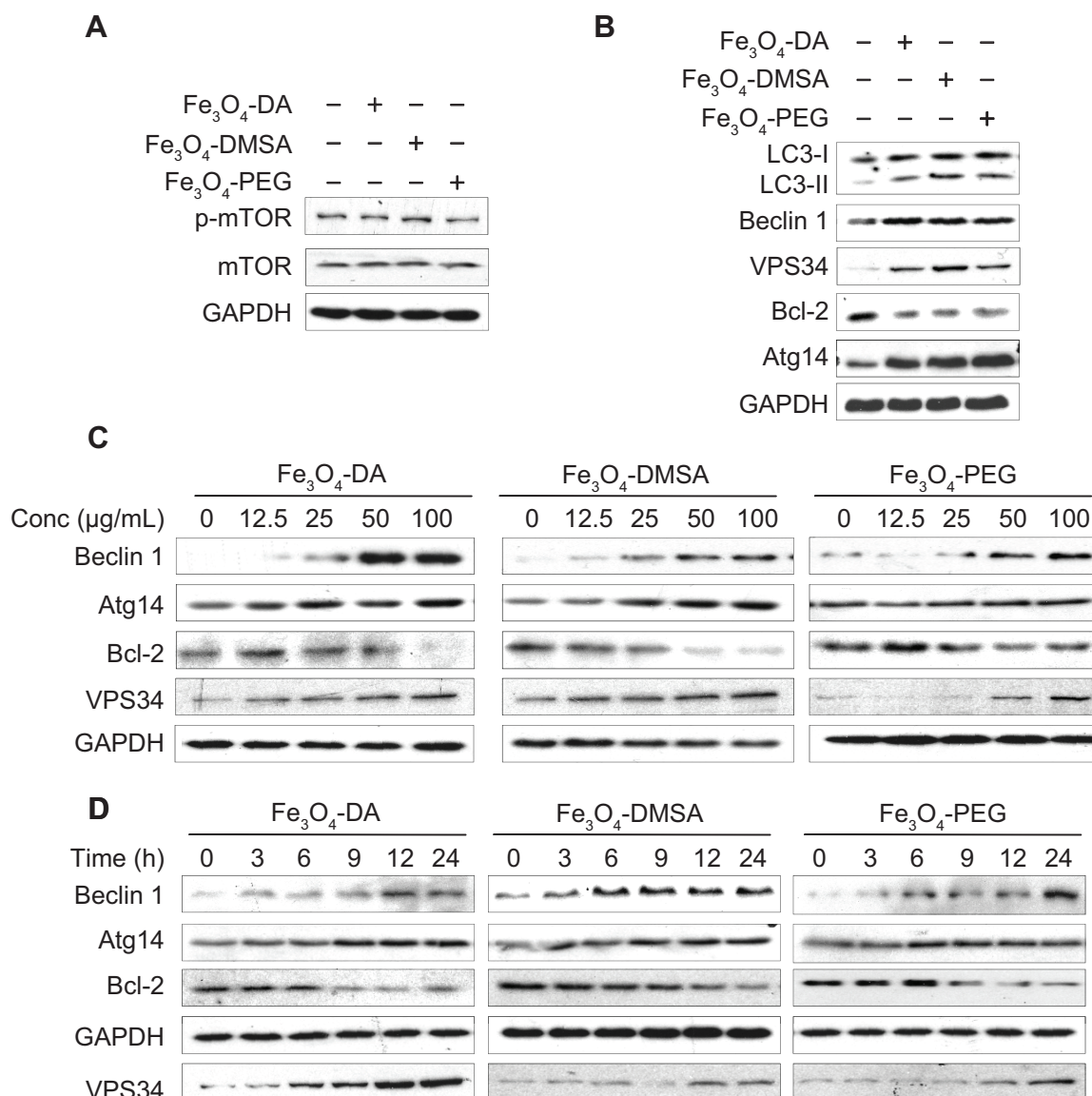


**Figure 4** Chemically modified Fe<sub>3</sub>O<sub>4</sub> NPs upregulate the expression of the Beclin 1/Atg14/VPS34 complex.

**Notes:** (A) OPM2 cells were treated Fe<sub>3</sub>O<sub>4</sub> NPs (100 µg/mL) for 9 hours followed by measurement of mTOR signals. (B) After treatment, OPM2 cells were subjected to immunoblotting for Beclin 1, Bcl-2, VPS34, and Atg14. (C) OPM2 cells were treated with Fe<sub>3</sub>O<sub>4</sub> NPs (100 µg/mL) for 9 hours at increasing concentrations as indicated. (D) OPM2 cells were treated with Fe<sub>3</sub>O<sub>4</sub> NPs (100 µg/mL) at increasing incubation time periods as indicated.

**Abbreviations:** BafA, bafilomycin A1; DA, dopamine; DMSA, dimercaptosuccinic acid; Fe<sub>3</sub>O<sub>4</sub>, ferrous oxide; GAPDH, glyceraldehyde-phosphate dehydrogenase; LC3, light chain 3; mTOR, mammalian target of rapamycin; NPs, nanoparticles; PEG, polyethyleneglycol; p-mTOR, phosphorylated mammalian target of rapamycin.

cancer cells, all these Fe<sub>3</sub>O<sub>4</sub> NPs led to increased expression of LC3-II and Beclin 1, and downregulated the expression of Bcl-2 in the primary healthy blood cells (Figure 7). These results indicated that Fe<sub>3</sub>O<sub>4</sub> NPs also induced autophagy in primary healthy blood cells.

## Discussion

The present study showed that Fe<sub>3</sub>O<sub>4</sub> NPs, both bare and surface modified forms, induce autophagy in both healthy and malignant blood cells although they failed to provoke apoptosis in these cells, which was confirmed by the

increased LC3-II expression, LC3-II containing puncta, the degradation of the protein p62, upregulation of the Beclin 1/VPS34/Atg14 complex, and the cleavage of apoptotic markers PARP and caspase-3.

Autophagy is a conserved cellular response to the changes in their living circumstances, and it is usually activated by various chemical, physical, or biological stresses. Upon activation, autophagy can act as a cell survival mechanism or as a route to cell death depending on the circumstances. For example, in the deprivation of nutrients, cells are undergoing autophagy, which recycles

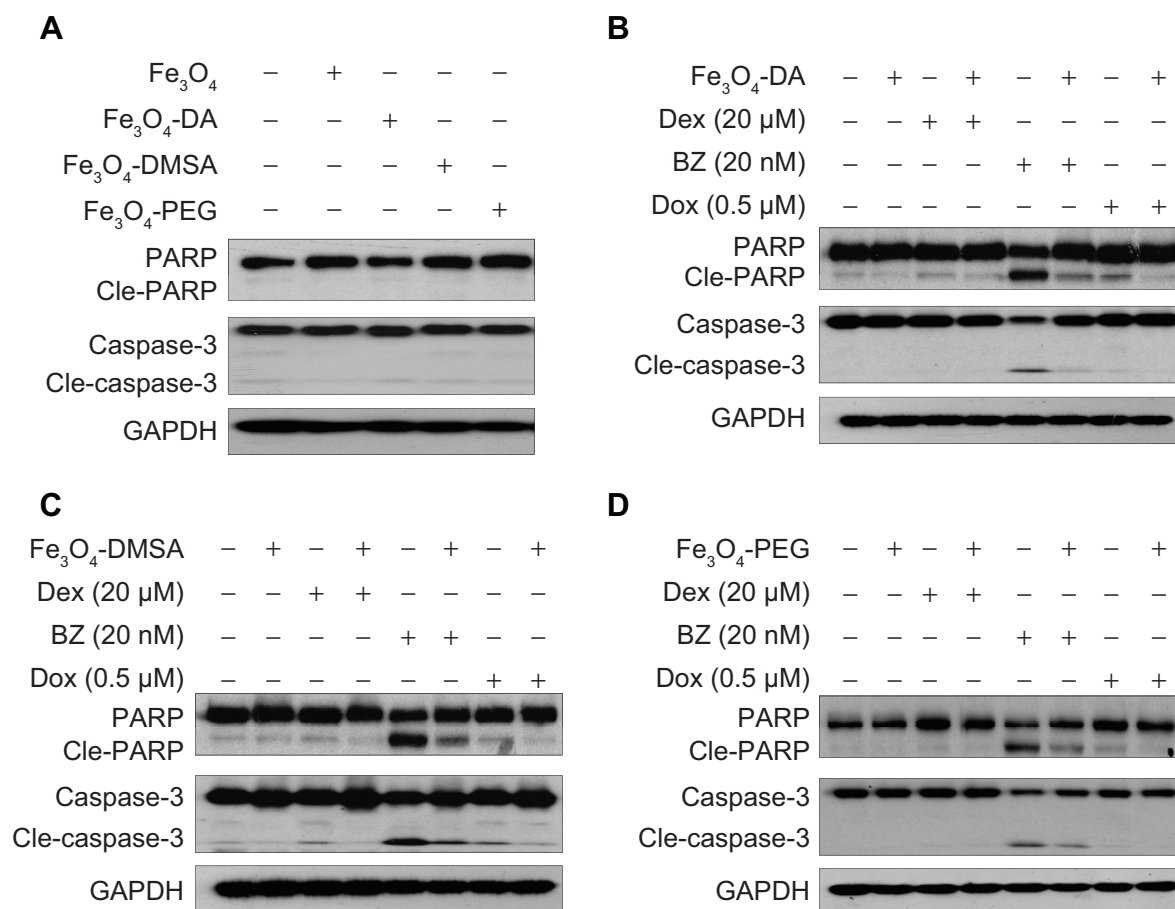


**Figure 5** Fe<sub>3</sub>O<sub>4</sub> NPs abolish apoptosis induced by anticancer drugs.

**Notes:** (A) OPM2 cells were treated indicated nanoparticles (100 μg/mL) for 9 hours, followed by measurement of PARP and caspase-3, hallmarks of apoptosis. (B) OPM2 cells were cotreated with Fe<sub>3</sub>O<sub>4</sub>-DA, (C) Fe<sub>3</sub>O<sub>4</sub>-DMSA, or (D) Fe<sub>3</sub>O<sub>4</sub>-PEG and Dex (20 μM), BZ (20 nM), or Dox (0.5 μM) for 9 hours, followed by analysis of PARP and caspase-3.

**Abbreviations:** BZ, bortezomib; DA, dopamine; Dex, dexamethasone; Dox, doxorubicin; DMSA, dimercaptosuccinic acid; Fe<sub>3</sub>O<sub>4</sub>, ferroferric oxide; GAPDH, glyceraldehyde-phosphate dehydrogenase; NPs, nanoparticles; PARP, poly ADP-ribose polymerase; PEG, polyethyleneglycol.

essential amino acids or fatty acids for their survival. Although some nanoparticles are believed to be biocompatible, it may vary depending on the nature of nanoparticles themselves and the cell types. For example, silica nanoparticles and CdSe/ZnS quantum dots can induce autophagy in A549 cells<sup>6</sup> in synapse,<sup>18</sup> respectively. In our present study, we found Fe<sub>3</sub>O<sub>4</sub> NPs activate autophagy in both normal and malignant blood cells. Nanoparticle-induced autophagy may be associated with the core nanoparticle or the surface modifications because sometimes the surface modifications lead to activated biological activities of the particles. A recent study showed that polystyrene nanoparticles with amino groups (PS-NH<sub>2</sub>) but not with carboxyl groups (PS-DMSA) rapidly induce autophagy in human leukemia cells, which suggests the surface modifications are important for autophagy induction.<sup>19</sup> In our study, all bare, negatively and positively modified Fe<sub>3</sub>O<sub>4</sub> NPs induce autophagy, suggesting that the surface

coating on Fe<sub>3</sub>O<sub>4</sub> NPs may not be a key factor in terms of autophagy induction.

There are three major pathways to regulate autophagy initiation: (1) the mammalian target of rapamycin (mTOR) that negatively regulates autophagy; (2) the Beclin 1/VPS34/Atg14 complex and (3) two ubiquitin-like conjugation processes that generate membrane-bound protein complexes, promoting the formation of LC3-conjugated autophagosome.<sup>20</sup> In our study, we found that inhibition of mTOR by Fe<sub>3</sub>O<sub>4</sub> NPs is not marked, suggesting that mTOR signaling control is not critical for autophagy induced by Fe<sub>3</sub>O<sub>4</sub> NPs. Because 3-MA can partly abolish Fe<sub>3</sub>O<sub>4</sub> NP-induced autophagy, the Beclin 1/VPS34/Atg14 complex might be involved in the induction of autophagy induced by Fe<sub>3</sub>O<sub>4</sub> NPs. This hypothesis is also supported by the induction of Beclin 1 and Atg14 and by the decreased Bcl-2 expression even at 24 hours after treatment with Fe<sub>3</sub>O<sub>4</sub> NPs. Notably, these changes are accompanied by increased LC3-II and decreased p62. Beclin 1 is the



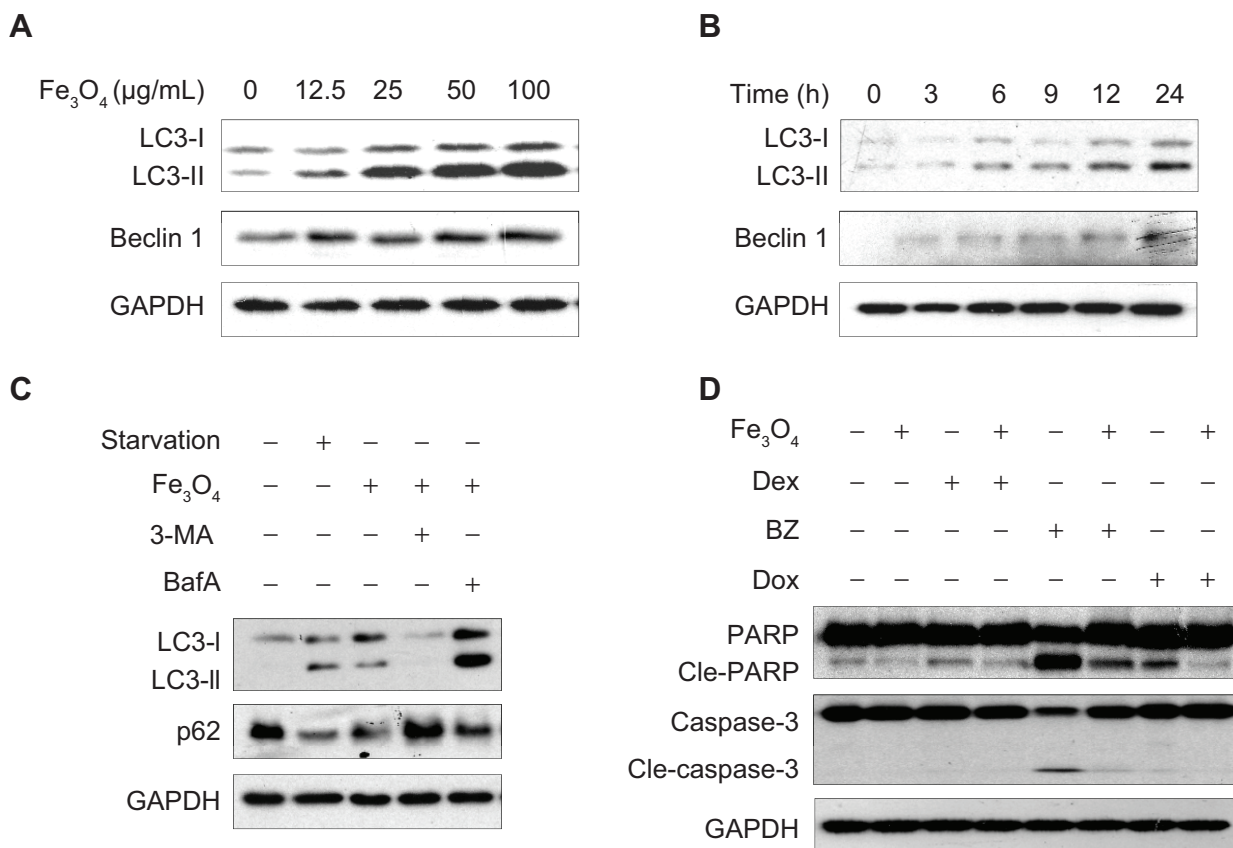


**Figure 6** Bare Fe<sub>3</sub>O<sub>4</sub> NPs induce prosurvival autophagy.

**Notes:** (A) OPM2 cells were treated with bare Fe<sub>3</sub>O<sub>4</sub> NPs in different concentrations for 9 hours or (B) 100 μg/mL of bare Fe<sub>3</sub>O<sub>4</sub> NPs at indicated time periods followed by LC3 and Beclin 1 analyses. (C) OPM2 cells were treated with bare Fe<sub>3</sub>O<sub>4</sub> NPs alone or along with 3-MA or BafA for 9 hours, followed by LC3 and p62 analysis. (D) OPM2 cells were treated with bare Fe<sub>3</sub>O<sub>4</sub> NPs alone or along with anticancer drugs Dex (20 μM), BZ (20 nM), or Dox (0.5 μM) for 9 hours, followed by analysis of apoptotic biomarkers PARP and caspase-3.

**Abbreviations:** 3-MA, 3-methyladenine; BafA, bafilomycin A1; BZ, bortezomib; Dex, dexamethasone; Dox, doxorubicin; Fe<sub>3</sub>O<sub>4</sub>, ferrous oxide; GAPDH, glyceraldehyde-phosphate dehydrogenase; LC3, light chain 3; NPs, nanoparticles; PARP, poly ADP-ribose polymerase.

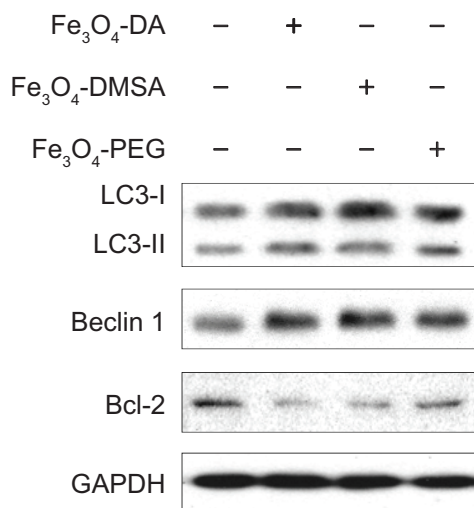


**Figure 7** Fe<sub>3</sub>O<sub>4</sub> NPs induce autophagic signaling in normal peripheral blood cells.

**Notes:** Nucleated cells isolated from peripheral blood of male mice were incubated with Fe<sub>3</sub>O<sub>4</sub> NPs (100 μg/mL) for 9 hours followed by immunoblotting against LC3, Beclin 1, and Bcl-2 with specific antibodies.

**Abbreviations:** Bcl-2, B-cell lymphoma 2; DA, dopamine; DMSA, dimercaptosuccinic acid; Fe<sub>3</sub>O<sub>4</sub>, ferrous oxide; GAPDH, glyceraldehyde-phosphate dehydrogenase; LC3, light chain 3; NPs, nanoparticles; PEG, polyethyleneglycol.

mammalian homologous of yeast Atg6, which plays a key role in the process of autophagy.<sup>21</sup> In intact cells, Beclin 1 forms a complex with Bcl-2; therefore Bcl-2 acts as an inhibitor of autophagy.<sup>22</sup> In the stimulations of autophagy, the protein level of Beclin 1 is increased while that of Bcl-2 is decreased, Beclin 1 thus dissociates from Bcl-2, and, in turn, it binds to and forms an active complex with VPS34 and Atg14 and promotes the progression of autophagy.<sup>22</sup> In our study, Fe<sub>3</sub>O<sub>4</sub> NPs decreased the expression of Bcl-2 but increased the expression of both Beclin 1 and Atg14 in a time- and concentration-dependent manner, further suggesting autophagy induced by these Fe<sub>3</sub>O<sub>4</sub> NPs are highly associated with the Beclin 1/Bcl-2/Atg14/VPS34 complex.

Lastly, Autophagy is considered to induce a double-faced effect on cell activity (e.g. cell death or survival), depending on the context. We found that the Fe<sub>3</sub>O<sub>4</sub> NPs prevent cytotoxicity induced by some anticancer drugs such as BZ, suggesting that these NPs prefer to display a prosurvival effect and that autophagy induced by these NPs

assists to recycle amino acids and other nutrients essential for cell survival. Notably, this effect was also observed in other healthy and malignant cells. Because the blood system is probably the most exposed system to these NPs in their medical application, either as a contrast in imaging or a format in preparation of anticancer drugs, caution should be taken especially when these NPs are used for blood cancer patients.

In summary, our study demonstrated that Fe<sub>3</sub>O<sub>4</sub> NPs can induce the autophagy in blood cells by regulating the Beclin 1/Bcl-2/Atg14/VPS34 complex. Fe<sub>3</sub>O<sub>4</sub> NPs are not toxic but display prosurvival activity in blood cells. Whether these particles affect other systems is yet to be determined.

## Acknowledgments

This investigation was partly supported by the National Basic Research Program of China (2011CB933501), the National Natural Science Foundation of China (Grant No 81101795, 81272632, 81320108023), the Priority Academic Program Development of Jiangsu Higher Education Institutions (PAPD), and Jiangsu Key Laboratory of Translational Research and Therapy for Neuro-Psycho-Diseases (BM2013003).

## Disclosure

None of the authors has a conflict of interest with this work.

## References

- Chen H, Wang L, Yu Q, et al. Anti-HER2 antibody and ScFvEGFR-conjugated antifouling magnetic iron oxide nanoparticles for targeting and magnetic resonance imaging of breast cancer. *Int J Nanomedicine*. 2013;8:3781–3794.
- Ghazani AA, Pectasides M, Sharma A, et al. Molecular characterization of scant lung tumor cells using iron-oxide nanoparticles and micro-nuclear magnetic resonance. *Nanomedicine*. 2014;10:661–668.
- Yokoyama T, Tam J, Kuroda S, et al. EGFR-targeted hybrid plasmonic magnetic nanoparticles synergistically induce autophagy and apoptosis in non-small cell lung cancer cells. *PLoS One*. 2011;6(11):e25507.
- Couto D, Freitas M, Vilas-Boas V, et al. Interaction of polyacrylic acid coated and non-coated iron oxide nanoparticles with human neutrophils. *Toxicol Lett*. 2014;225:57–65.
- Halamoda Kenzaoui B, Chapuis Bernasconi C, Guney-Ayra S, Juillerat-Jeanneret L. Induction of oxidative stress, lysosome activation and autophagy by nanoparticles in human brain-derived endothelial cells. *Biochem J*. 2012;441:813–821.
- Nowak JS, Mehn D, Nativo P, et al. Silica nanoparticle uptake induces survival mechanism in A549 cells by the activation of autophagy but not apoptosis. *Toxicol Lett*. 2014;224:84–92.
- Cheng L, Yang K, Li Y, et al. Facile preparation of multifunctional upconversion nanoprobes for multimodal imaging and dual-targeted photothermal therapy. *Angew Chem Int Ed Engl*. 2011;50(32):7385–7390.
- Arsianti M, Lim M, Marquis CP, Amal R. Assembly of polyethylenimine-based magnetic iron oxide vectors: insights into gene delivery. *Langmuir*. 2010;26:7314–7326.
- Jahn MR, Shukoor I, Tremel W, et al. Hemin-coupled iron(III)-hydroxide nanoparticles show increased uptake in Caco-2 cells. *J Pharm Pharmacol*. 2011;63:1522–1530.
- Wu Y, Song M, Xin Z, et al. Ultra-small particles of iron oxide as peroxidase for immunohistochemical detection. *Nanotechnology*. 2011;22: 225703.
- Zhang J, Tang J, Cao B, et al. The natural pesticide dihydrorotenone induces human plasma cell apoptosis by triggering endoplasmic reticulum stress and activating p38 signaling pathway. *PLoS One*. 2013;8: e69911.
- Cao B, Li J, Zhou X, et al. Clotrimazole induces pro-death autophagy in leukemia and myeloma cells by disrupting the mTOR signaling pathway. *Sci Rep*. 2014;4:5749.
- Mao X, Cao B, Wood TE, et al. A small-molecule inhibitor of D-cyclin transactivation displays preclinical efficacy in myeloma and leukemia via phosphoinositide 3-kinase pathway. *Blood*. 2011;117:1986–1997.
- Ni HM, Bockus A, Wozniak AL, et al. Dissecting the dynamic turnover of GFP-LC3 in the autolysosome. *Autophagy*. 2011;7:188–204.
- Mizushima N, Yoshimori T, Levine B. Methods in mammalian autophagy research. *Cell*. 2010;140:313–326.
- Moscat J, Diaz-Meco MT. p62 at the crossroads of autophagy, apoptosis, and cancer. *Cell*. 2009;137:1001–1004.
- Yang Z, Klionsky DJ. Eaten alive: a history of macroautophagy. *Nat Cell Biol*. 2010;12:814–822.
- Chen L, Miao Y, Chen L, et al. The role of elevated autophagy on the synaptic plasticity impairment caused by CdSe/ZnS quantum dots. *Biomaterials*. 2013;34:10172–10181.
- Loos C, Syrovets T, Musyanovych A, Mailänder V, Landfester K, Simmet T. Amino-functionalized nanoparticles as inhibitors of mTOR and inducers of cell cycle arrest in leukemia cells. *Biomaterials*. 2014; 35:1944–1953.
- Itakura E, Kishi C, Inoue K, Mizushima N. Beclin 1 forms two distinct phosphatidylinositol 3-kinase complexes with mammalian Atg14 and UVRAG. *Mol Biol Cell*. 2008;19:5360–5372.
- Kang R, Zeh HJ, Lotze MT, Tang D. The Beclin 1 network regulates autophagy and apoptosis. *Cell Death Differ*. 2011;18:571–580.
- Marquez RT, Xu L. Bcl-2:Beclin 1 complex: multiple, mechanisms regulating autophagy/apoptosis toggle switch. *Am J Cancer Res*. 2012;2: 214–221.

International Journal of Nanomedicine

Publish your work in this journal

The International Journal of Nanomedicine is an international, peer-reviewed journal focusing on the application of nanotechnology in diagnostics, therapeutics, and drug delivery systems throughout the biomedical field. This journal is indexed on PubMed Central, MedLine, CAS, SciSearch®, Current Contents®/Clinical Medicine,

Submit your manuscript here: <http://www.dovepress.com/international-journal-of-nanomedicine-journal>

Dovepress

Journal Citation Reports/Science Edition, EMBASE, Scopus and the Elsevier Bibliographic databases. The manuscript management system is completely online and includes a very quick and fair peer-review system, which is all easy to use. Visit <http://www.dovepress.com/testimonials.php> to read real quotes from published authors.